

## Supporting Information

# Surface Engineering of Mitigating Compressive Stress and Detrimental Reactions for NiO<sub>x</sub>-based Inverted Perovskite Solar Cells

Zijin Qiao,<sup>#a</sup> Hongye Dong,<sup>#a</sup> Guibin Shen,<sup>b</sup> Xiangning Xu,<sup>a</sup> Wang Yao<sup>a</sup>, Cheng Mu<sup>\*a</sup>

Table S1 Device performance on the concentration of SB12-3 solution

Concentration (mg / mL)	$V_{OC}$ (V)	$J_{SC}$ (mA cm <sup>-2</sup> )	Fill factor (FF)	PCE (%)
0	1.050	21.07	0.766	16.94
0.25	1.076	22.12	0.764	18.18
0.5	1.084	22.32	0.782	18.92
1	1.087	21.54	0.747	17.51

Table S2 Device performance without SB12-3 modification.

Concentration (mg / mL)	$V_{OC}$ (V)	$J_{SC}$ (mA cm <sup>-2</sup> )	Fill factor (FF)	PCE (%)
1	1.064	21.14	0.708	15.92
2	1.064	20.41	0.704	15.29
3	1.065	21.25	0.730	16.53
4	1.044	21.42	0.710	15.88
5	1.051	20.44	0.708	15.20
6	1.052	20.79	0.745	16.30
7	1.049	20.62	0.763	16.49
8	1.042	21.31	0.723	16.04
9	1.040	21.12	0.760	16.69
10	1.045	21.37	0.741	16.54
11	1.062	20.28	0.723	15.48
12	1.052	20.79	0.760	16.30
13	1.049	20.61	0.741	16.49
14	1.043	21.33	0.719	16.79
15	1.040	21.31	0.745	16.15
16	1.060	20.58	0.701	15.38
17	1.066	20.45	0.737	16.06
18	1.036	21.01	0.702	15.27
19	1.052	20.22	0.712	15.15
20	1.063	21.32	0.747	16.70
21	1.060	20.29	0.748	16.08
22	1.060	21.75	0.724	16.68
23	1.069	20.90	0.730	16.31
24	1.067	20.23	0.743	16.05
25	1.064	20.02	0.739	15.73
26	1.064	21.16	0.732	16.48
27	1.074	20.32	0.715	15.60
28	1.066	19.71	0.722	15.16
29	1.054	20.07	0.732	15.48
30	1.046	20.67	0.734	15.87

Table S3 Device performance with SB12-3 modification

Concentration (mg / mL)	$V_{OC}$ (V)	$J_{SC}$ (mA cm <sup>-2</sup> )	Fill factor (FF)	PCE (%)
1	1.073	21.37	0.745	17.09
2	1.081	21.47	0.742	17.21
3	1.083	21.41	0.731	16.95
4	1.072	21.18	0.746	16.93
5	1.060	21.67	0.756	17.36
6	1.083	22.32	0.782	18.92
7	1.073	21.90	0.771	18.12
8	1.083	22.05	0.780	18.61
9	1.082	21.85	0.734	17.36
10	1.089	21.83	0.743	17.66
11	1.083	21.66	0.730	17.13
12	1.077	21.77	0.739	17.30
13	1.084	21.70	0.738	17.37
14	1.068	21.26	0.753	17.10
15	1.083	21.19	0.764	17.54
16	1.090	21.80	0.721	17.13
17	1.087	21.76	0.727	17.19
18	1.086	22.66	0.743	18.28
19	1.087	22.72	0.736	18.17
20	1.078	21.76	0.712	16.69
21	1.088	21.68	0.729	17.21
22	1.083	22.16	0.716	17.18
23	1.082	22.30	0.725	17.49
24	1.084	22.09	0.714	17.09
25	1.084	22.14	0.719	17.25
26	1.079	21.03	0.781	17.71
27	1.085	22.47	0.712	17.32
28	1.083	21.99	0.733	17.47
29	1.076	21.42	0.772	17.78
30	1.073	21.54	0.755	17.46

Table S4. Time constants of the fast ( $\tau_1$ ) and slow ( $\tau_2$ ) decay components obtained from the TRPL spectra of the perovskite films.

Sample	$\tau_1$ (ns)	$A_1$	$\tau_2$ (ns)	$A_2$	$\tau_{\text{avg}}$ (ns)
NiO <sub>x</sub>	138.9	0.44	1391	0.32	1253.60
NiO <sub>x</sub> / SB12-3	19.74	25.44	1175.78	0.34	854.08

The average lifetime can be calculated with the equation of:  $\tau_{\text{avg}} = (A_1\tau_1^2 + A_2\tau_2^2) / (A_1\tau_1 + A_2\tau_2)$ . Here,  $\tau_1$  and  $\tau_2$  represent trap-assisted and free carrier recombination, respectively,  $A_1$  and  $A_2$  represent the decay amplitude.

Table S5.  $V_{\text{TFL}}$  and  $N_t$  from the space charge limited current measurements of the hole-only devices.

Devices	$\epsilon_0$ ( $\times 10^{-12}$ F m <sup>-1</sup> )	$\epsilon$	$V_{\text{TFL}}$ (V)	$e$ ( $\times 10^{-19}$ C)	$L$ (nm)	$N_t$ ( $\times 10^{15}$ cm <sup>-3</sup> )
NiO <sub>x</sub>	8.85	26	0.25	1.6	715	1.40
NiO <sub>x</sub> / SB12-3	8.85	26	0.16	1.6	715	0.39

The trap density  $N_t$  is defined as:

$$N_t = 2\epsilon\epsilon_0 V_{\text{TFL}} / eL^2$$

Here,  $\epsilon_0$  is the vacuum permittivity,  $\epsilon$  is the relative dielectric constant,  $e$  is the elementary charge, and  $L$  is the thickness of perovskite film.

Table S6. Fitting parameters of TPV curve with different devices.

Sample	$\tau_1$ ( $\mu$ s)	$A_1$	$\tau_2$ ( $\mu$ s)	$A_2$	$\tau_{\text{avg}}$ ( $\mu$ s)
NiO <sub>x</sub>	4.74	0.30	12.71	0.17	8.19
NiO <sub>x</sub> / SB12-3	7.55	0.94	36.04	0.04	12.36

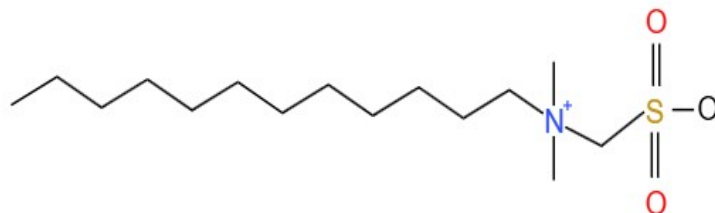


Figure S1 Molecule structure of SB12-3.

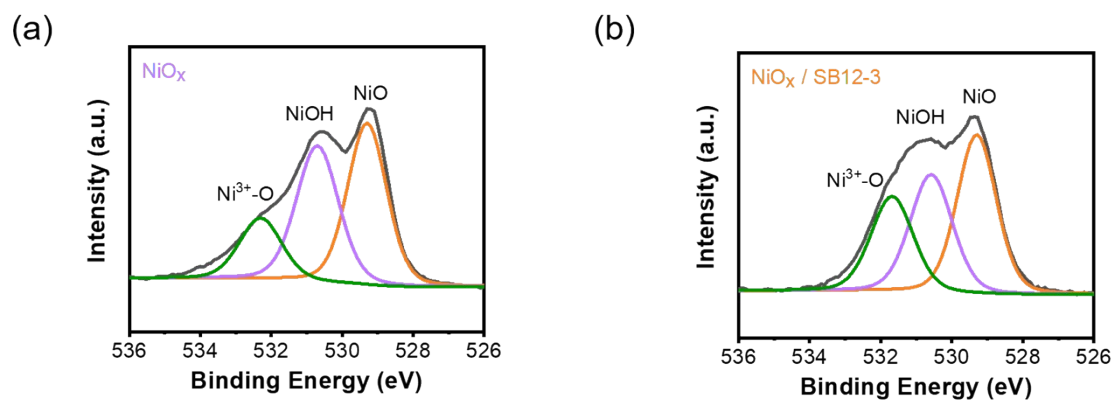


Figure S2. XPS spectra of O 1s for (a) NiO<sub>x</sub> and (b) NiO<sub>x</sub>/SB12-3.

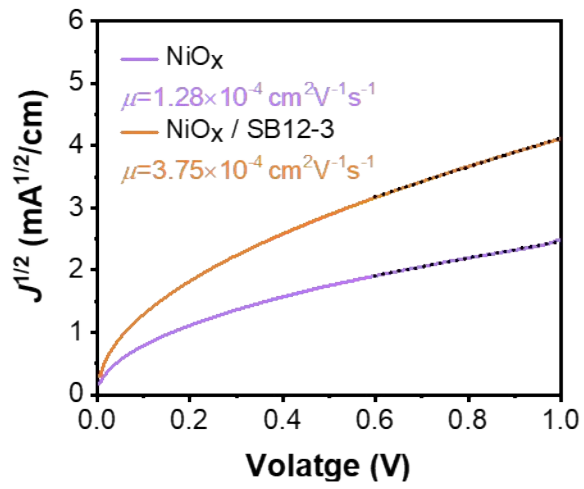


Figure S3: Electron mobility curves of NiO<sub>x</sub> and NiO<sub>x</sub>/SB12-3.

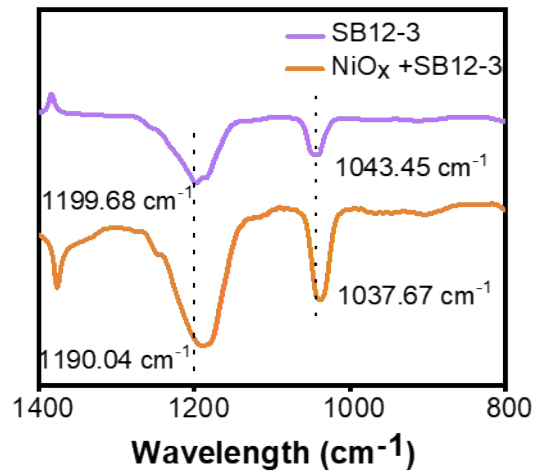


Figure S4: Fourier transform infrared (FTIR) spectra of NiO<sub>x</sub> with or w/o SB12-3.

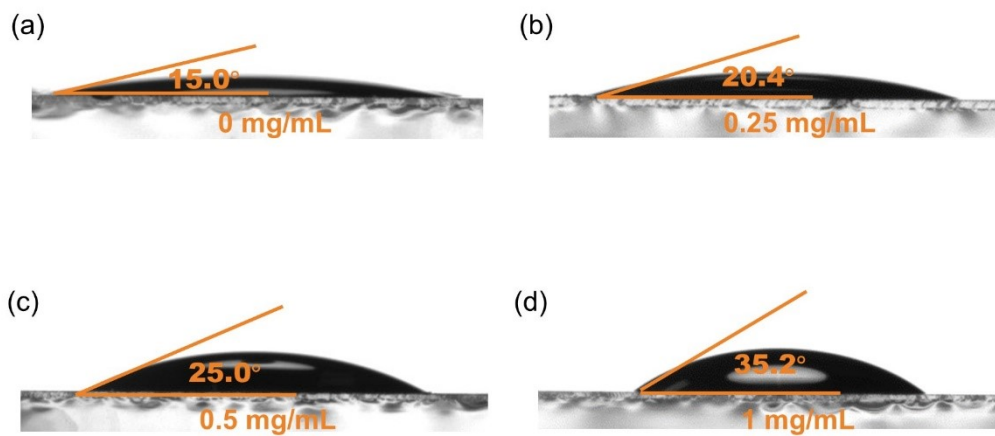


Figure S5: The contact angles of perovskite solution deposited on NiO<sub>x</sub> layer with different concentration of SB12-3 solution.

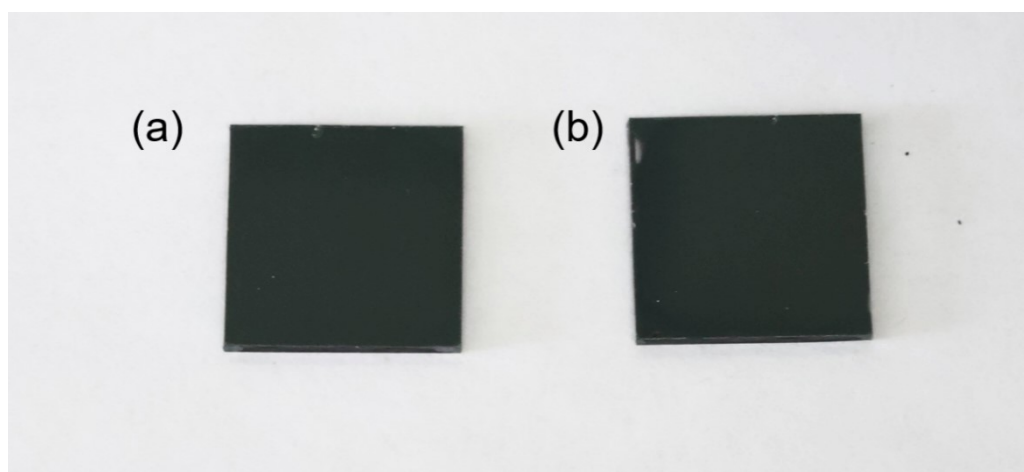


Figure S6: Fabricated film photographs of the (a) NiO<sub>x</sub>/perovskite and (b) NiO<sub>x</sub>/0.5mg/mL SB12-3/perovskite.

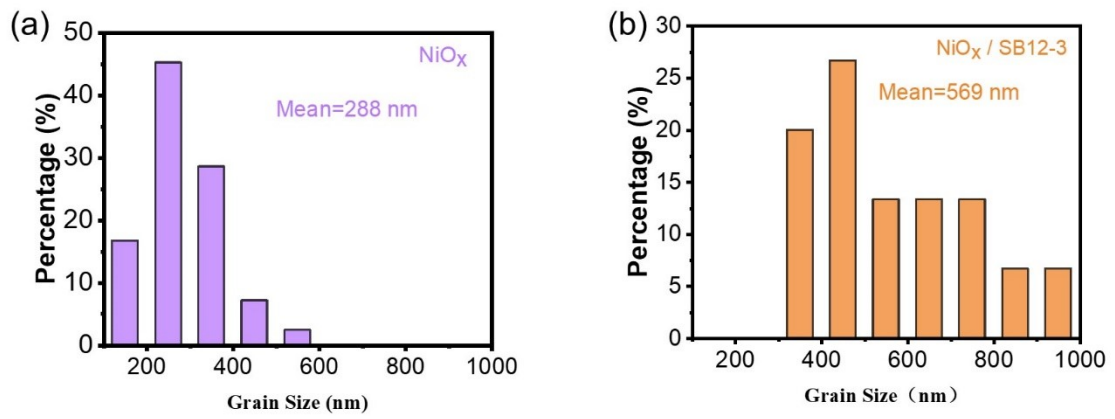


Figure S7 : Histogram of grain size distribution corresponding to the top-view SEM of perovskite films deposited on (a)  $\text{NiO}_x$  and (b)  $\text{NiO}_x/\text{SB12-3}$ .

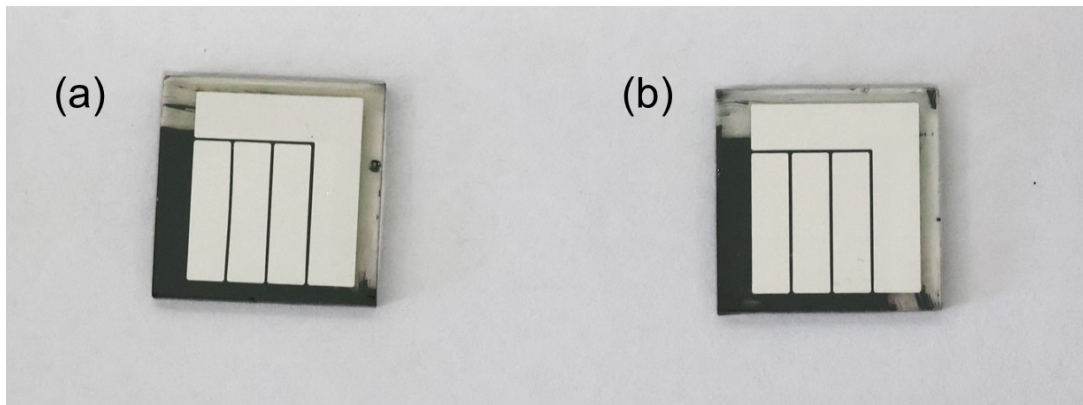


Figure S8: Device photographs of the (a)  $\text{NiO}_x$  and (b)  $\text{NiO}_x/\text{SB12-3}$  PSCs.

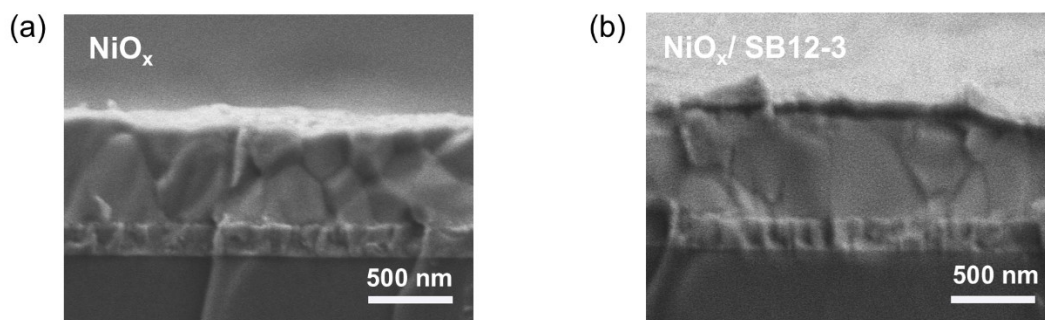


Figure S9: Cross-sectional SEM images of the (a)  $\text{NiO}_x$  and (b)  $\text{NiO}_x / \text{SB12-3}$  PSCs.

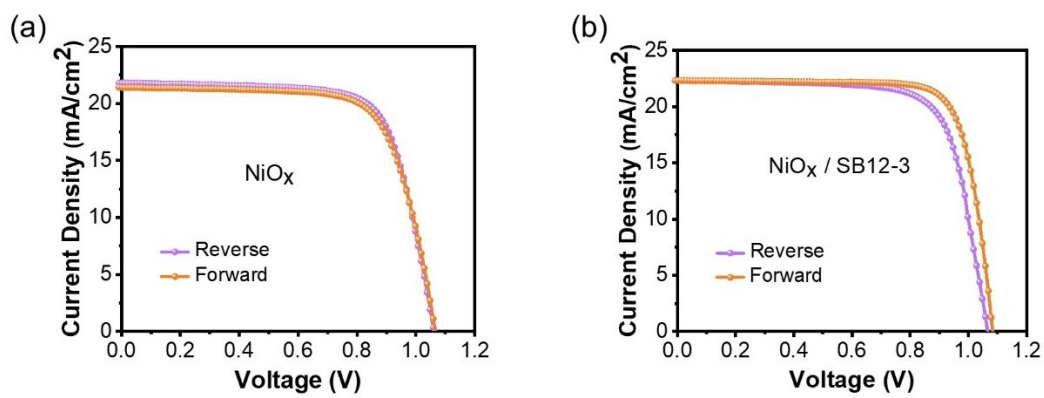


Figure S10: J-V curves of the control and modified PSCs measured in forward and reverse scans.

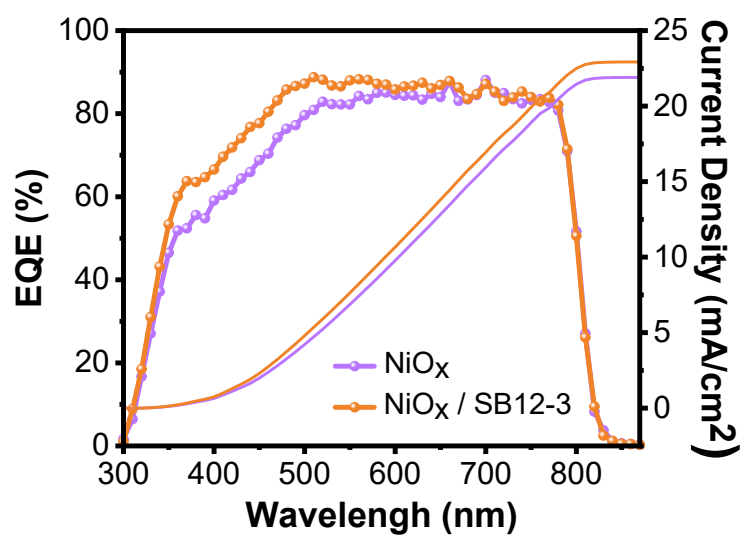


Figure S11: EQE spectra and the corresponding integrated  $J_{SC}$ .

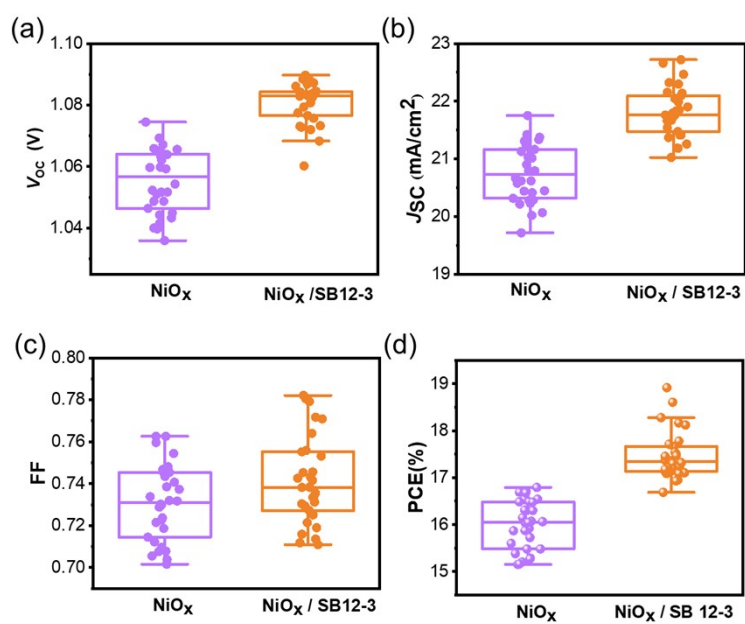


Figure S12: Statistical distribution of  $V_{OC}$  (a);  $J_{SC}$  (b); FF (c) and PCE(d) for 30 devices.

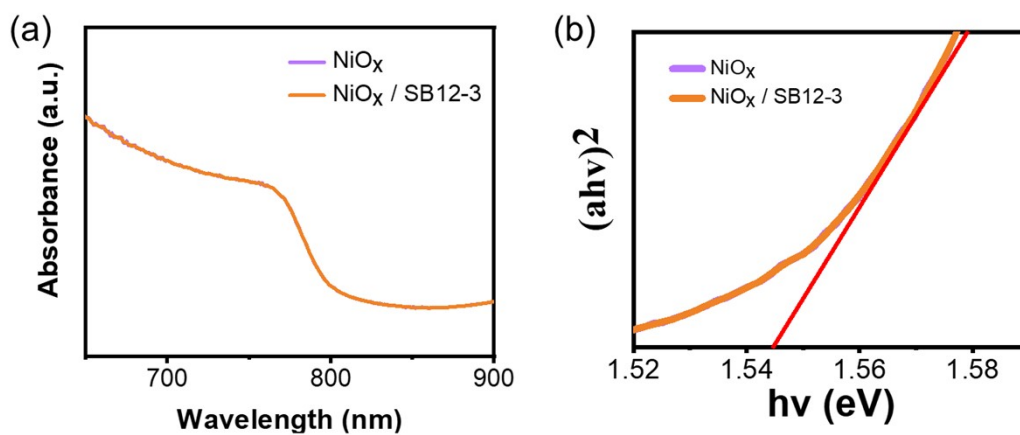


Figure S13: (a) UV-Vis absorption spectra of perovskite films deposited on  $\text{NiO}_x$  and  $\text{NiO}_x / \text{SB12-3}$ , (b) Tauc plot of perovskite films at  $\text{NiO}_x$  and  $\text{NiO}_x / \text{SB12-3}$  layer.